

Charge Carriers in Few-Layer Graphene Films

Sylvain Latil and Luc Henrard

Laboratoire de Physique du Solide, Facultés Universitaires Notre-Dame de la Paix, rue de Bruxelles 61, 5000 Namur, Belgium
(Received 8 March 2006; published 19 July 2006)

The nature of the charge carriers in 2D few-layer graphites (FLGs) has been recently questioned by transport measurements [K. S. Novoselov *et al.*, *Science* **306**, 666 (2004)] and a strong ambipolar electric field effect has been revealed. Our density functional calculations demonstrate that the electronic band dispersion near the Fermi level, and consequently the nature of the charge carriers, is highly sensitive to the number of layers and the stacking geometry. We show that the experimentally observed ambipolar transport is only possible for an FLG with a Bernal-like stacking pattern, whereas simple-carrier or semiconducting behavior is predicted for other geometries.

DOI: [10.1103/PhysRevLett.97.036803](https://doi.org/10.1103/PhysRevLett.97.036803)

PACS numbers: 81.05.Uw, 71.15.Mb, 73.90.+f

The recent transport measurements in monocrystalline graphite containing only a few layers (called few-layer graphite or FLG) have demonstrated their potential technological importance in semiconductor applications, due to gate control of the transport properties. These 2D structures (they contain up to a dozen shells) are produced either by peeling a highly oriented pyrolytic graphite deposited on SiO₂ [1], or by heating a SiC thin film [2]. More recently, the existence of *massless* fermions, with a linear dispersion relation, has also been reported [3] in single layer graphene (SLG).

The bulk 3D graphites are semimetallic materials that exhibit very peculiar electronic properties. Indeed, the first semiempirical models for Bernal (or AB) [4] and rhombohedral (or ABC) graphites [5] have demonstrated that the shape of the Fermi surface, and consequently the nature of the charge carriers, is strongly dependent upon the geometry of the stacking between layers. The Fermi surfaces of the both structures are located at the edge of the Brillouin zones (BZs) and exhibit a complex shape, due to the coexistence of holes and electrons at the Fermi level. *Ab initio* calculations have latterly confirmed these statements [6,7].

In contrast to the corresponding three-dimensional (3D) bulk structures, electrons in a FLG are confined along one crystallographic direction, offering a genuine 2D character to its electronic response. First studies of transport in FLGs have been carried out and the nature of the charge carriers, as well as their effective masses, have been determined by Hall measurements. FLGs have been shown to behave like mixed carriers semimetallic systems, with a domain of coexistence of electrons and holes [1,2]. Moreover, the fact that they switch from electron to hole transport by when a gate voltage is applied, as well as their particularly long mean-free path ($\ell \approx 0.4 \mu\text{m}$), makes FLGs remarkable workbenches for both mesoscopic transport studies and low dimensional physics. Indeed, this ability of tuning the transport properties by an external electrostatic potential is a key issue of modern nanoelectronics.

A detailed understanding of the experimental data of Ref. [1] has, however, been hindered by the incomplete knowledge of the sample geometry. If AFM measurement showed that the maximum number of layers should be 4, it gives no information on the stacking. A simple two-band model was proposed, based mainly on the value of the overlap $\delta\varepsilon$ between hole and electron bands. This is a crucial parameter that determines the gate potential needed to switch between electron and hole conduction, and consequently drives the electronic transport. Experimental results indicate that the value of $\delta\varepsilon$ varies from 4 to 20 meV, but do not allow conclusions to be made on the stacking order.

In this Letter, the electronic properties of 2D few-layer graphites are further investigated using first principle techniques. FLGs 2D crystals belong to an intermediate design between bulk graphite and a graphene plane, so their band structures will be reminiscent of both of them. The weak interlayer interaction that creates the band dispersion out of the basal plane in 3D graphites is now responsible for the band mixing (between isolated SLG bands) occurring in FLGs. Since coexistence of carriers is only possible when different bands are present in the same energy range, the number of layers and the geometry dependence of the interlayer interaction are key parameters influencing the transport properties of FLGs. Indeed, it is shown below that, depending of the case, a FLG can be metallic (with single or mixed carriers) or a narrow-gap semiconducting 2D system.

The structures studied in this work were made from one to four layers and assumed to be isolated (the substrate was neglected), and to have a hexagonal lattice. Hence, the turbostratic situation was not studied, but is discussed in the conclusion. Since the simple hexagonal (AA) graphite is energetically unfavored [8], we have avoided this stacking when building up the set of studied FLGs. In this situation the only bilayer structure is the AB, presented in Fig. 1. With three layers, two different isomers are possible: ABA and ABC (Fig. 1). Four-layered structures

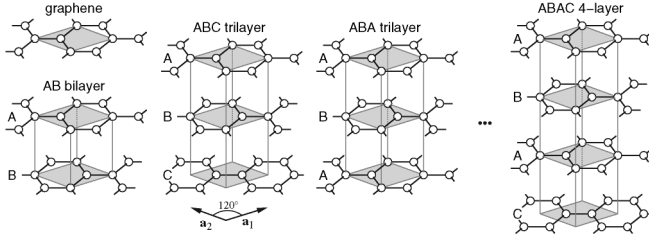


FIG. 1. The 2D primitive cells of some FLGs.

are, respectively, ABAB, ABCA (not shown) and ABAC (identical to ABCB, Fig. 1).

The electronic properties were investigated using the ABINIT density functional code [9], within the local density approximation (LDA) scheme. This numerical technique, in spite of not explicitly accounting for the van der Waals part of the interlayer interaction, has been proved to give the correct equilibrium structure and to be accurate enough to tackle the complex band structure of 3D graphites in the vicinity of E_F [7,10]. A norm-conserving pseudopotential was used for the carbon element [11], and the plane wave basis set was given a cutoff energy $E_{\text{cut}} = 35$ Ha. Integrations over the BZ are based on a 30×30 Monkhorst-Pack 2D grid [12] ensuring the convergence of Kohn-Sham states (Γ , K , and M special points are included) and the structures were optimized prior to the electronic study [13].

First, the band structure of the single layer graphene is reproduced in Fig. 2(a). Its space group contains a mirror plane symmetry, allowing symmetric σ and antisymmetric π bands to be distinguished [14]. SLG is then characterized by the linear dispersion of the π bands near E_F , that can represent *massless* fermions. Their electronic group velocities, estimated at the crossing point, is high: 8.4×10^5 m \cdot s $^{-1}$. When several SLGs interact to form a FLG, the former antisymmetric π bands are split (owing to bonding or

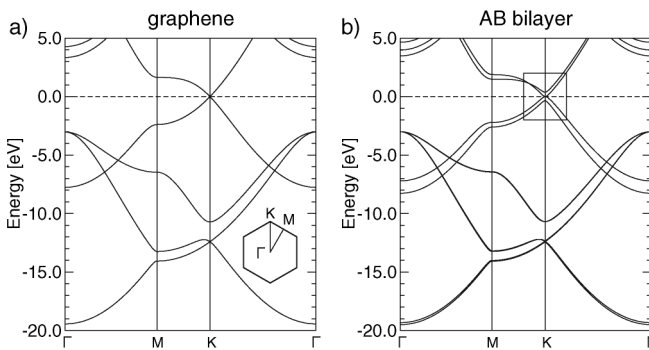


FIG. 2. (a) The band structure of a single graphene layer shows the remarkable linear dispersion of the π bands at Fermi level $E_F = 0$, in the vicinity of K (the Brillouin zone is shown in inset). (b) When two graphene layers are stacked and interact, a band splitting occurs, and the linear dispersion is lost. The square indicates the domain that is magnified in Fig. 3.

antibonding patterns) whereas the σ ones are much less affected, as shown for an AB bilayer in Fig. 2(b). Bands of FLGs containing more layers behave similarly (not shown). Magnification of the band structure plot, in the vicinity of the K point, is presented in Fig. 3 for the complete set of studied FLGs.

The valence band (VB) and conduction band (CB) of the AB bilayer [Fig. 3(a)] only admit two contact points, avoiding any deep domain of coexistence of electrons and holes. The reason is the symmetry group of the AB bilayer ($P\bar{3}m1$) does not contain the horizontal mirror plane, so VB and CB can not be degenerated, except along high-symmetry axes. The close-up of the overlapping region, drawn in Fig. 4(a), gives a comprehensive scheme of this statement: in spite of their parabolic shape along the high-symmetry axes the curve's “extrema” are actually saddle points (delimiting a pseudogap $\epsilon_{\text{psg}} = 2.6$ meV) and the real overlap between the two touching points (K itself and one point along the $K\Gamma$ axis) is $\delta\epsilon = 0.8$ meV. This domain of coexistence is far too narrow to be visible experimentally. None ambipolar transport would be reported in this case contrary to the measure published by Novoselov *et al.* [1]. Moreover, the electronic group velocities estimated on these contact points is much lower than for SLG ($< 10^5$ m \cdot s $^{-1}$), giving poor conducting properties to the AB bilayer (by comparison to graphene).

From the AB bilayer, the ABC trilayer is constructed with an additional layer, keeping the same stacking pattern. It can be seen as the first precursor of the rhombohedral graphite and defines a “rhombohedral family” (FLGs with a ABCAB ... stacking geometry which belongs to the $P\bar{3}m1$ space group). The band structure of the ABC trilayer is plotted in Fig. 3(b) and shows a single crossing point between VB and CB, located on the KM axis. As a consequence, any coexistence of charge carriers is strictly forbidden in this case. However, a graphene quasi-*massless* dispersion exists, as sketched in Fig. 4(b). It is bounded by a pseudogap $\epsilon_{\text{psg}} = 18$ meV. The group velocities in this domain vary from 1.9 to 2.6×10^5 m \cdot s $^{-1}$. We turn now to the ABCA 4-layer graphite, continuing with the same stacking geometry. Its band structure [Fig. 3(c)] is very similar to the bilayer graphite: two bands join the Fermi level and allow only a few crossing points (K , and one point on the KM axis). Group velocities at these points are in a range from 0.5 to 1.2×10^5 m \cdot s $^{-1}$. Now, the pseudogap is $\epsilon_{\text{psg}} = 4.8$ meV and the net overlap between VB and CB is $\delta\epsilon = 2.1$ meV [Fig. 4(c)]: still too narrow to be compared with the results already published. Finally, the band structure of rhombohedral stacked FLGs does not exhibit any measurable domain of coexistence of carriers, and is characterized by a pseudogap bounded by saddle points.

The “Bernal family” differs from the previous case, as it brings together FLGs with ABABA ... stacking. The band structure of the ABA trilayer, shown in Fig. 3(d), is char-

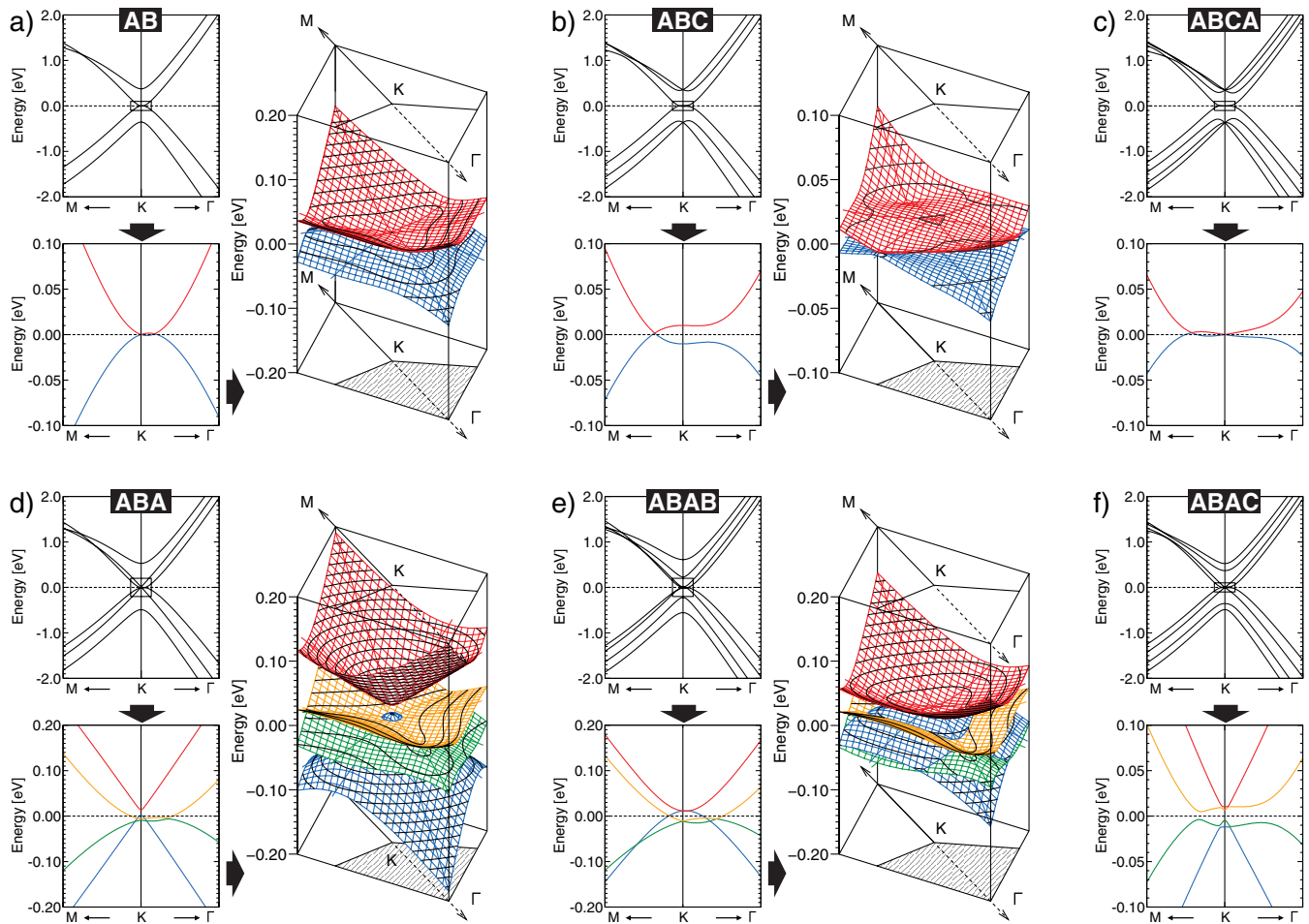


FIG. 3 (color). Details of FLGs band structure in the vicinity of K , and near the Fermi level (always set as zero). (a) The valence band (VB, in blue) and the conduction band (CB, in red) of an AB trilayer exhibit a clear trigonal shape around K . They admit crossing points only along high-symmetry axis. (b) In the case of an ABC trilayer, there is one contact point, located on the KM high-symmetry axis. (c) A similar situation occurs for the ABCA 4-layer graphite. VB and CB admit discrete crossing points. (d) The ABA trilayer presents a net crossing of bands, not only along high-symmetry axes, but for any point around K , creating a domain of coexistence of electrons (orange) and holes (blue). It is also characterized by the quasilinear dispersion of bands (blue and red). (e) On the same way, the ABAB 4-layer presents crossing between a hole band (blue) and an electron band (orange). (f) The bands of the ABAC 4-layers are not crossing (even along high-symmetry axes) and a gap is open.

acterized by band crossings in the vicinity of the Fermi level. Notice that this crossing defines a contour around the K point in the BZ (as shown in the 3D plot), and does not occur only along high-symmetry axes. In fact, the space group of the ABA trilayer ($P6m2$) again contains the horizontal mirror symmetry, allowing it to separate the antisymmetric states [orange and green in Fig. 3(d)] and the symmetric ones (blue and red). Moreover, the two symmetric bands exhibit a quasi linear dispersion (*massless fermions*); however, unlike the SLG, a gap opens due to the nonequivalence of carbon atoms in a same layer ($\varepsilon_{\text{gap}} = 12.1$ meV). The band overlap between the top of the quasi *massless* holes band (blue) and the electrons band (orange) is $\delta\varepsilon_1 = 8.0$ meV for the first valley, and $\delta\varepsilon_2 = 5.4$ meV for the second [shown in Fig. 4(d)].

Continuing with the Bernal stacking, we studied the ABAB 4-layer graphite. Similarly to the previous case, its band structure presents crossings [Fig. 3(e)] allowing a net overlap between a hole band (plotted in blue) and an electron band (in orange). The schematic close-up, drawn in Fig. 4(e), gives a comprehensive point of view; the overlap with the first valley is $\delta\varepsilon_1 = 22.6$ meV, and with the second valley $\delta\varepsilon_2 = 17.6$ meV. It is important to notice that, contrary to the ABA trilayer, the ABAB *does not* have any horizontal mirror symmetry (the space group of Bernal FLGs with an even number of layers is $P\bar{3}m1$), so the crossing behavior can not be explained by symmetry arguments [15]. It appears then that the Bernal-like (ABABA...) is the best kind of stacking for explaining the ambipolar transport, since electrons and holes coexist

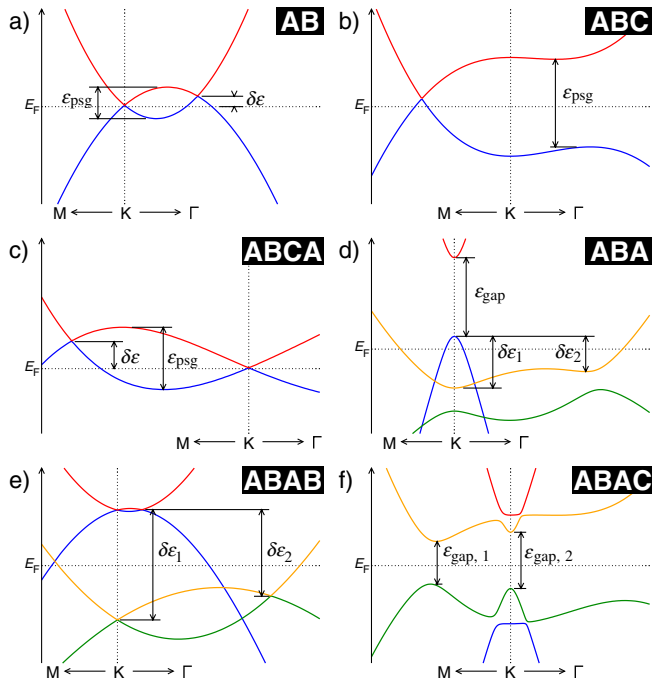


FIG. 4 (color online). Schematic close-up of the bands at E_F . The AB bilayer (a) the ABC trilayer (b) and the ABCA 4-layer (c) do not exhibit any significant overlap $\delta\epsilon$ and present a pseudogap ϵ_{psg} . On the other hand, a large domain of coexistence is found for the ABA trilayer (d) and the ABAB 4-layer (e). Differently to the previous cases, the ABAC 4-layer (f) exhibits a gap.

in these structures, for a sufficiently wide domain of energy.

Lastly, we complete our overview of the few-layer graphites with the ABAC 4-layer graphite, which is related to neither the rhombohedral nor Bernal geometries. As shown in Fig. 3(f), the band structure does not exhibit any crossing nor contact point, even along high-symmetry directions. This 2D crystal is a narrow-gap semiconductor, with a quasidirect gap $\epsilon_{\text{gap},1} = 8.8$ meV. A secondary gap is also present $\epsilon_{\text{gap},2} = 11.5$ meV, as sketched in Fig. 4(f).

Beside these perfectly stacked structures, FLG made by turbostraticlike stacking should be examined. In fact, such a structure will not belong to any symmetry, so the presence of a significant band overlap is very unlikely. Moreover, the larger interlayer distance would strongly reduce the electronic dispersion perpendicular to the basal plane. We then do not think that the coexistence of charge carriers can be measurable in a nonsymmetric structure like a turbostratic FLG.

In conclusion, we have shown that the geometry of stacking and the number of layers of a few layers graphite strongly affects its band structure in the region of the Fermi level and, consequently, its transport properties. We then theoretically demonstrated that the field effect behaviors observed by Novoselov *et al.* are intrinsic properties of

ABA trilayer and ABAB 4-layer FLG systems. We found, however, that these band structures are much richer than the simple two-band model. Other structures, like the bilayer or the rhombohedral-like trilayer and 4-layer, do not rise to any deep overlap of hole and electron bands. They are also characterized by the presence of saddle points near the Fermi level that are predicted to drive an orbital paramagnetism [16]. Lastly, the ABAC 4-layer structure presents a gap in the Terahertz range that could be probed by microwave measurements.

We are grateful to J.-C. Charlier for sharing his knowledge on the physical properties of graphites, and to S. Roche and Ph. Lambin for valuable discussions and remarks. The present work was carried out within the framework of the Belgian IAP Program No. P5/01 *quantum size effects in nanostructured materials*. S. L. acknowledges the Francqui Foundation of Belgium for financial subsidies and L. H. is supported by the Belgian FNRS.

- [1] K. S. Novoselov *et al.*, Science **306**, 666 (2004).
- [2] C. Berger *et al.*, J. Phys. Chem. B **108**, 19912 (2004).
- [3] K. S. Novoselov *et al.*, Nature (London) **438**, 197 (2005); Y. Zhang *et al.*, Nature (London) **438**, 201 (2005).
- [4] J. W. McClure, Phys. Rev. **108**, 612 (1957); J. C. Slonczewski and P. R. Weiss, Phys. Rev. **109**, 272 (1958).
- [5] R. R. Haering, Can. J. Phys. **36**, 352 (1958); J. W. McClure, Carbon **7**, 425 (1969).
- [6] G. S. Painter and D. E. Ellis, Phys. Rev. B **1**, 4747 (1970); D. Tománek and S. G. Louie, Phys. Rev. B **37**, 8327 (1988).
- [7] J.-C. Charlier, X. Gonze, and J.-P. Michenaud, Phys. Rev. B **43**, 4579 (1991); Carbon **32**, 289 (1994).
- [8] J. C. Charlier, J. P. Michenaud, and X. Gonze, Phys. Rev. B **46**, 4531 (1992).
- [9] X. Gonze *et al.*, Comput. Mater. Sci. **25**, 478 (2002).
- [10] Energy scale reaches the limit of the LDA (~ 10 meV); the numerical values of the results should be regarded as semiquantitative.
- [11] N. Troullier and J. L. Martins, Phys. Rev. B **43**, 8861 (1991).
- [12] H. J. Monkhorst and J. D. Pack, Phys. Rev. B **13**, 5188 (1976).
- [13] The atomic displacement involved during optimizations were smaller than 10^{-3} Å. The cell parameter was found to be rather the same for all the structures $a = 2.4507$ Å. The value of c was fixed to 24 Å, avoiding any self-interaction of the slabs.
- [14] In a 2D crystal, a parallel mirror symmetry operation separates the eigenstates for all the BZ, and not only along some high-symmetry axis.
- [15] A closer study of the dispersion indicates that an avoided crossing occurs actually between the hole band [plotted in orange on Fig. 3(e)] and the electron band (in blue). Since the energy scale of this gap opening is tiny (< 0.1 meV), and for reasons of clarity, we have assumed that it is a true crossing when drawing the band structure.
- [16] G. Vignale, Phys. Rev. Lett. **67**, 358 (1991).